16th Mediterranean Conference on Control and Automation
Congress Centre, Ajaccio, France
June 25-27, 2008

Mechatronic Design and Position Control of a Novel Ball and Plate System

Miad Moarref, Mohsen Saadat, and Gholamreza Vossoughi, *Member, IEEE*

Abstract—**The mechatronic design of a novel mechanism for ball and plate system is discussed. A webcam provides the system with feedback of the ball's position. A heuristic technique for image processing is introduced. The kinematics and dynamics of the system are also described. Supervisory fuzzy control and sliding control techniques are proposed to perform position control for the system. Experimental results corroborate the validity of the controllers.**

I. Introduction

THE *ball and plate* system is a generalization of the famous *ball and beam* benchmark. The latter is a two Degree of Freedom system consisting of a ball that can roll on a rigid beam, while the former is a four DOF system consisting of a ball that can roll freely on a rigid plate. Despite worldwide recognition of the ball and beam system as a control benchmark and existence of numerous publications on the topic [1], the ball and plate system has not attracted that much attention. Although, the difficulty of creating a ball and plate mechanism with respect to a ball and beam mechanism is the main drawback of such systems, the enormous potential of performing manifold control strategies on ball and plate systems make them desirable. The ball and plate system can be an appropriate device for studying control techniques at graduate level.

A few ball and plate systems have been produced before. The mechatronic design of a ball and plate system that takes advantage of a spatial mechanism for rotating the plate is described in [2]. However, the mechanism suffers from an undesirable third DOF which is plate's rotation in its own plane. In that work, a PID controller that is based on the linearized model of the system is used to control the ball's position. The ball and plate system in [3] is designed for educational purposes and performs tracking control via geometric control and PID controllers. Reference [4] uses a robot manipulator as the actuation mechanism and applies sliding control method to the linearized model to control the ball. HUMUSOFT [5] is a tendon drive ball and plate mechanism that is commercially available. This device was used in [6] and [7] for tracking control using fuzzy control methods.

The main contributions of this paper are introduction of a novel mechanism for the ball and plate system and implementation of new control techniques.

In this paper, a novel mechanism for the ball and plate system is presented. The spatial parallel mechanism enables the plate to rotate about two perpendicular axes while maintaining a fixed point at the center of the plain. Moreover, both actuators are located on the base and thus minimize the device's inertia. Other advantages of this mechanism include high stiffness and minor backlash.

For sensing the ball's position and receiving (sending) signals from sensors (to actuators), a webcam and an ADVANTECH PCI-1753 data acquisition card are used respectively.

This paper is organized as follows. Section II introduces the ball and plate mechanism and compares it with other mechanisms available in literature. The kinematic and dynamic equations of the system are provided in Section III. Next, fuzzy and nonlinear techniques for control of the ball and plate system are presented. In Section V, experimental results are illustrated. Concluding remarks are provided in Section VI.

II. Mechatronics of the Ball and Plate System

The main mechatronic features of the ball and plate system are discussed in this section. They include the actuation mechanism, ball's position sensing strategies, and real-time control.

A. Actuation Mechanism

The actuation mechanism implemented for the ball and plate system is inspired by [8]. It consists of a five link spatial parallel mechanism where the links are connected to each other via five one DOF rotational joints (see Fig. 1).

The benefits of this mechanism include:

1) Actuators are located on the base of the mechanism. It lessens the inertia of this device, as opposed to the mechanism where one actuator rotates the plate along one direction and the second actuator which is located on the base turns both the plate and the second actuator.

2) The heuristic arrangement of joints' rotation axes provides the mechanism with a fixed point O (see Fig. 2) which simplifies deriving the ball's equations of motion and control signals. The mechanism introduced in [2] lacks this characteristic.

3) This mechanism has higher stiffness and lower backlash, contrary to tendon drive mechanisms such as [5].

Two five-phase stepper motors are used as actuators. The

Manuscript received February 3, 2008.

M. Moarref, M. Saadat, and Gh. Vossoughi are with the Mechanical Engineering Department, Sharif University of Technology, Tehran, 11365-9567 IRAN (phone: (+98) 917-315-0617; e-mail: moarref@ mech.sharif.ir).

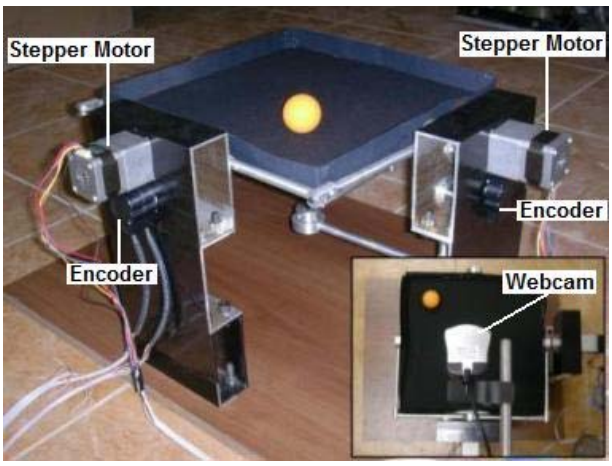

Fig. 1. The ball and plate mechanism.

innate characteristics of a stepper motor provide the opportunity to control the plate's angular position directly. They also make the dynamic equations of the system independent of the plate's dynamics. Considering the angular velocity of the two stepper motors as inputs, the system looses two of its degrees of freedom and becomes a *squared system*.

Due to stepper motors' sporadic missing of steps, one can not rely on them for measuring angle of rotation. Thus, in this system optical encoders are implemented to measure the angles of rotation of the stepper motors. These data are used to calculate the plate's angular position. The relations between plate's angular position and actuators' angle of rotation are derived in Section III.

B. Ball's Position Sensing Method

The position of the ball is extracted from pictures taken by a webcam (Fig. 1) using MATLAB's image acquisition and image processing toolboxes. This sensing method is clearly cheaper than the touch-screen sensor used in [2].

The procedure for finding the ball on a grabbed picture consists of the following steps:

1) The picture is converted to a bi-level image. This Image can be regarded as a matrix whose elements are either one (white) or zero (black). Imagine that the ball appears as a white circle in a black plane in this bi-level image.

2) The sum of elements in each row and column of the image are calculated.

3) The row and column with the largest sum of elements correspond to the point located at the center of the ball.

In order to speedup the process of taking and analyzing pictures, the *dynamic window method* is implemented. Using this method, only a small portion of each frame that is located around the ball's estimated position is searched, as opposed to searching the full camera frame. Assume that at time t_k the ball's center is at (x_k, y_k) and the ball is moving with velocity $(\dot{x}_k, \dot{y}_k)$, then the corners of the dynamic camera window at time t_{k+1} will be at $\left(x_k + \dot{x}_k (t_{k+1} - t_k) \pm l/2, y_k + \dot{y}_k (t_{k+1} - t_k) \pm w/2\right)$ where l and w are the length and width of the dynamic camera window respectively.

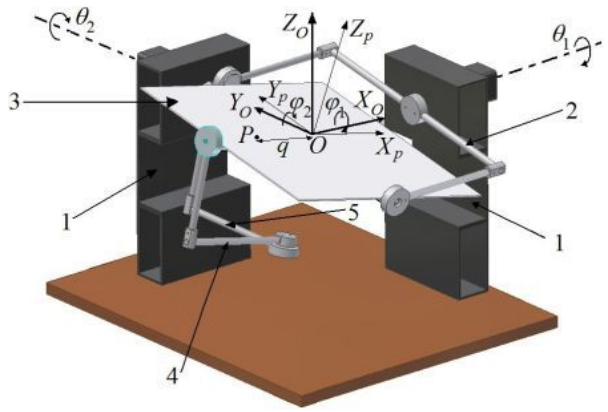

Fig. 2. The ball and plate mechanism. The numbers show the mechanism's five links. The frame with index O is fixed to the base and the frame with index p is fixed to the plate.

Using this method, the whole process of sensing the ball's location can be done in less than 0.05 seconds on a regular PC.

C. Real-Time Control

ADVANTECH PCI-1753 data acquisition card is used for generating and sending signals to stepper motors and receiving data from encoders. The control process is done in MATLAB using real-time windows target toolbox.

III. Kinematic and Dynamic Equations

Kinematic relations between plate angles φ_1 and φ_2 and actuators angles θ_1 and θ_2 are provided in this section as well as the equations of motion of the ball.

A. Kinematic Relations

Since the plate is directly connected to the first actuator (see Fig. 2), the kinematic relation between plate's angle φ_1 and the first actuator's angle θ_1 is given by the trivial equation $\varphi_1 = \theta_1$.

In order to find a relation between φ_2 and the two actuator angles, an inversion of the mechanism is implemented. In this inversion link 2 is considered as the base of the mechanism instead of link 1. Next, an arbitrary point P is selected between point O and the joint between links 3 and 4, and the mechanism is virtually broken through this point. Using the smaller part of the mechanism one can find the position of point P by equation:

$$P = \begin{bmatrix} q \sin\varphi_2 \\ 0 \\ q \cos\varphi_2 \end{bmatrix} \quad (1)$$

where q is the distance between P and the fixed point O.

Implementing the notations and conventions introduced in

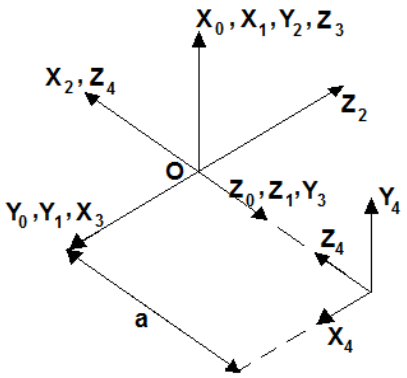

Fig. 3. Link frame assignment [9]. a is the distance between point O and the joint between links 3 and 4.

[9], one can calculate the position of point P using the larger part of the mechanism. Fig. 3 illustrates the frames assigned to each link. Denavit-Hartenberg parameters are shown in Table I. Position of point P is derived as follows:

$$P=\begin{bmatrix} -q\left(\cos\theta_1\sin\theta_2\cos\theta_3-\sin\theta_1\sin\theta_3\right) \\ -q\left(\sin\theta_1\sin\theta_2\cos\theta_3+\cos\theta_1\sin\theta_3\right) \\ q\cos\theta_2\cos\theta_3 \end{bmatrix} \tag{2}$$

where θ_3 is the angle between links 4 and 5. Solving equations (1) and (2) for φ_2 one gets:

$$\varphi_2=\arctan\left(\frac{\tan\theta_2}{\cos\theta_1}\right) \tag{3}$$

B. Dynamic Equations

The ball's equations of motion are derived using Lagrange equations:

$$\frac{d}{dt}\left(\frac{\partial L}{\partial\dot{q}_i}\right)-\frac{\partial L}{\partial q_i}=Q_i \tag{4}$$

where q_i are the generalized coordinates (here x and y) and $L=T-U$, in which T and U are the kinetic and potential energies respectively.

The resulting equations of motion are fully coupled and contain manifold nonlinear terms:

$$\begin{aligned} \ddot{y}&=f_1(X)+\sum_{j=1}^{2}b_{1j}(X)\ddot{\theta}_j \\ \ddot{x}&=f_2(X)+\sum_{j=1}^{2}b_{2j}(X)\ddot{\theta}_j \end{aligned} \tag{5}$$

where $X=[x,\dot{x},y,\dot{y},\theta_1,\dot{\theta}_1,\theta_2,\dot{\theta}_2]^T$.

However, linearization of the system about plate's fixed point, leads to the following simple and decoupled equations:

$$\begin{aligned} \ddot{y}&=\tfrac{-5}{7}g\theta_1+R\ddot{\theta}_1 \\ \ddot{x}&=\tfrac{5}{7}g\theta_2-R\ddot{\theta}_2 \end{aligned} \tag{6}$$

In Section IV, these linearized, decoupled equations are used to create two similar but independent PID controllers for the system. The nonlinear equations of motion are also implemented to obtain a sliding control strategy for the system.

TABLE I
DENAVIT-HARTENBERG PARAMETERS

i	α_{i-1}	a_{i-1}	d_i	θ_i
1	0	0	0	θ_1
2	$\pi/2$	0	0	$\pi/2+\theta_2$
3	$-\pi/2$	0	0	$\pi/2+\theta_3$
4	$\pi/2$	0	$-a$	θ_4

The parameters are introduced in details in [9]. θ_4 is the angle between links 3 and 4.

IV. POSITION CONTROL

In this section, two different methods for controlling the ball's position are presented. In the first approach, the linearized model is used to create a PID controller with a supervisory fuzzy controller which controls the PID gains. Next, the sliding control of the nonlinear system is discussed.

A. PID Controller with Supervisory Fuzzy Control

Recalling the linearized set of equations, it is clear that x is a function of θ_2 only. Similarly, y is a function of θ_1 only. In other words, the system can be treated as two different SISO systems operating simultaneously. Hence similar but independent PID controllers can be used for controlling each coordinate of the ball's motion.

First, a preliminary controller is designed using the *loop within a loop* scheme. Second, a supervisory fuzzy controller is designed to adjust the PID gains on-line. Fig. 4 shows a diagram of this controller.

A simple proportional controller is adequate to obtain the desired response from the inner loop, in which the encoder feedback is used to achieve servo position control. This inner loop is then placed in an outer loop that controls the ball's position. The outer loop controller is based on the transfer function between each of ball's position coordinates and its corresponding actuator's angular velocity, that is

$$\begin{aligned} \frac{y}{\dot{\theta}_1}&=\frac{\frac{-5}{7}g+Rs^2}{s^3} \\ \frac{x}{\dot{\theta}_2}&=\frac{\frac{5}{7}g-Rs^2}{s^3} \end{aligned} \tag{7}$$

Root-locus design technique was used to design an appropriate PD controller for the transfer functions.

The last step is to design a supervisory fuzzy system for tuning the PD controller gains with respect to ball's position error $e(t)$ and its time derivative $\dot{e}(t)$ [10]. Assuming that the outer loop controller is in the form of $K_p(1+K_d s)$, the fuzzy system adjusts this controller by changing the proportional and derivative gains (i.e. K_p and K_d) at each time step to achieve both fast response and small overshoot.

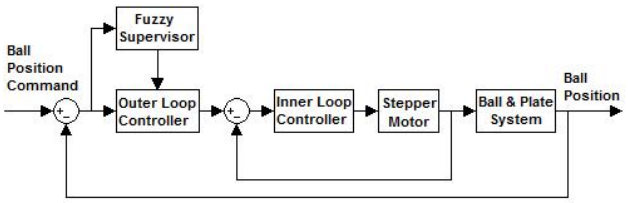

Fig. 4. The scheme of the PID loop within a loop controller and the supervisory fuzzy controller.

The fuzzy rules are derived experimentally based on the step response of the system. For example when $e(t)$ is large and $\dot{e}(t)$ is small, in order to have a fast rise time, a large proportional gain and a small derivative gain are needed. On the other hand, when $e(t)$ is small and $\dot{e}(t)$ is large, to avoid a large overshoot, a small proportional gain and a large derivative gain are desired.

For each PD controller, two fuzzy systems with two inputs (i.e. $e(t)$, $\dot{e}(t)$) and one output (each one of K_p and K_d) are designed. Seven normal, complete, and consistent triangular membership functions are defined on each input variable. Also, forty nine rules are defined on the output to make the fuzzy rule base complete. Note that the input and output variables of the fuzzy system were assumed to belong to the following sets: $e \in (-0.165, 0.165)$, $\dot{e} \in (-2.5, 2.5)$, $K_p \in (0.5, 4.5)$, and $K_d \in (0.5, 3)$.

The membership functions are illustrated in Fig. 5. Table II shows the set of rules for K_p. Similar sets of rules are produced for K_d.

The overall control scheme can be explained as follows: While the controller in the outer loop computes the angle by which the plate should move to balance the ball, the inner loop controller actually moves the plate by that angle. At the same time, the fuzzy system changes the PD controller gains to achieve a reasonable fast response with a small overshoot.

B. Sliding Control

Recalling (5), the nonlinear system is input to output linearized and its relative degree is (2, 2). The total relative degree of the system is 4, which is equal to the order of the system. Thus, one can be sure that the system does not have an unstable zero dynamics.

Assume $\mathbf{B}(X)$ is a matrix with elements b_{ij}. One can write:

$$\begin{bmatrix} \ddot{y} \\ \ddot{x} \end{bmatrix} = \begin{bmatrix} f_1(X) \\ f_2(X) \end{bmatrix} + \mathbf{B}(X) \begin{bmatrix} \ddot{\theta}_1 \\ \ddot{\theta}_2 \end{bmatrix} \tag{8}$$

The invertible matrix $\mathbf{B}(X)$ is often called the decoupling matrix, in the sense that the following decoupling control law

$$u = \begin{bmatrix} \ddot{\theta}_1 \\ \ddot{\theta}_2 \end{bmatrix} = \mathbf{B}^{-1}(X) \begin{bmatrix} w_1 - f_1(X) \\ w_2 - f_2(X) \end{bmatrix} \tag{9}$$

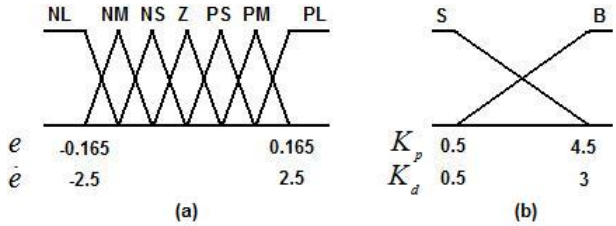

Fig. 5. (a) Membership functions for e and $\dot{e}$. (b) Membership functions for K_p and K_d.

TABLE II
SET OF FUZZY RULES FOR K_p

		e						
	μ	NL	NM	NS	Z	PS	PM	PL
	NL	S	B	B	B	B	B	S
	NM	S	S	B	B	B	S	S
	NS	S	S	S	B	S	S	S
$\dot{e}$	Z	S	S	S	S	S	S	S
	PS	S	S	S	B	S	S	S
	PM	S	S	B	B	B	S	S
	PL	S	B	B	B	B	B	S

can linearize the system.

To apply sliding control to this two input two output system, two sliding surfaces are introduced:

$$\begin{aligned} s_1 &= a_1 y + \dot{y} \\ s_2 &= a_2 x + \dot{x} \end{aligned} \tag{10}$$

which are stable for $a_1 > 0$ and $a_2 > 0$.

The equivalent control laws for moving along the sliding surfaces can be computed by the following equation:

$$\begin{bmatrix} u_{1eq} \\ u_{2eq} \end{bmatrix} = \mathbf{B}^{-1}(X) \begin{bmatrix} -f_1(X) - a_1 \dot{y} \\ -f_2(X) - a_2 \dot{x} \end{bmatrix} \tag{11}$$

Defining a Lyapunov function for the first surface, one can write derive a control law for reaching the sliding surface:

$$V_1 = \tfrac{1}{2} s_1^2 \Rightarrow \dot{V}_1 = s_1 \dot{s}_1 = s_1 [a_1 \dot{y} + f_1(X) + b_{11} u_1 + b_{12} u_2] \le -\eta_1 |s_1|$$

$$\text{sgn}(s_1)[a_1 \dot{y} + f_1(X) + b_{11} u_1 + b_{12} u_2] \le -\eta_1$$

$$u_1 = u_{1eq} - \tfrac{k_1}{b_{11}} \text{sgn}(s_1), k_1 \ge \eta_1 \tag{12.a}$$

where η_1 is a positive constant and the larger it is, the smaller is the reach time. A similar control law can be derived for the second surface:

$$u_1 = u_{1eq} - \tfrac{k_1}{b_{11}} \text{sgn}(s_1), k_1 \ge \eta_1 \tag{12.b}$$

As a result, the Lyapunov function $V = V_1 + V_2 = \tfrac{1}{2}(s_1^2 + s_2^2)$ with control signal (12) guarantees asymptotic stability of the origin.

From a control point of view, modeling inaccuracies can be classified into two major kinds: structured (or parametric) uncertainties and unstructured uncertainties (or un-modeled

dynamics). The first kind corresponds to inaccuracies on the terms actually included in the model, while the second kind corresponds to inaccuracies on (i.e., underestimation of) the system order [11].

In this paper, the following inaccuracies are assumed on system's parameters:

$$\begin{aligned} &-\pi/6 < \theta_1 < \pi/6, -\pi/6 < \theta_2 < \pi/6 \\ &-\pi/9 < \dot{\theta}_1 < \pi/9, -\pi/9 < \dot{\theta}_2 < \pi/9 \\ &0.01 < R < 0.02 \end{aligned} \quad (13)$$

where R is the ball's radius and its corresponding uncertainty is due to using balls with different radii in experiments.

The unstructured uncertainties include friction forces, actuator ripple, backlash and dither.

Considering these uncertainties and replacing the parameters with their nominal values, the equivalent control laws (11) are reduced to:

$$\begin{bmatrix} u_{1eq} \\ u_{2eq} \end{bmatrix} = \begin{bmatrix} -50\sqrt{2}\dot{y} \\ 50\sqrt{2}\dot{x} \end{bmatrix} \quad (14)$$

Defining the control signals to be in the form of

$$\begin{bmatrix} u_1 \\ u_2 \end{bmatrix} = \begin{bmatrix} u_{1eq} \\ u_{2eq} \end{bmatrix} + \begin{bmatrix} v_1 \\ v_2 \end{bmatrix} \quad (15)$$

one can write:

$$\begin{aligned} \dot{V}_1 &= s_1\dot{s}_1 = s_1[a_1\dot{y} + f_1(X) + b_{11}u_1 + b_{12}u_2] \\ &= s_1[a_1\dot{y} + f_1(X) + b_{11}(u_{1eq} + v_1) + b_{12}(u_{2eq} + v_2)] \\ &\le |s_1|[|a_1\dot{y}| + \max(f_1(X) + b_{11}u_{1eq} + b_{12}u_{2eq})] \\ &\quad + s_1[\min(b_{11})v_1 + \min(b_{12})v_2] \le -\eta_1|s_1| \end{aligned} \quad (16)$$

Writing similar relations for the second surface, one gets:

$$\begin{aligned} &\min(b_{11})v_1 + \min(b_{12})v_2 = \\ &\quad -(|a_1\dot{y}| + \max(f_1(X) + b_{11}u_{1eq} + b_{12}u_{2eq}) + \eta_1)\,\mathrm{sgn}(s_1) \\ &\min(b_{21})v_1 + \min(b_{22})v_2 = \\ &\quad -(|a_2\dot{x}| + \max(f_2(X) + b_{21}u_{1eq} + b_{22}u_{2eq}) + \eta_2)\,\mathrm{sgn}(s_2) \end{aligned} \quad (17)$$

The above equations can be used to compute the values of v_1 and v_2 which are in turn used to compute the control signals (15).

To avoid chattering, continuous function $sat(\frac{s_i}{\varphi_i})$ is used instead of the discontinuous function $\mathrm{sgn}(s_i)$. The new control laws guarantee that all trajectories will reach the boundary layer of thickness φ_i around the sliding surface s_i in finite time.

In order to increase the speed of computations, that is inevitable in real-time control applications, a fuzzy approximator system is used. The approximator comprises of two fuzzy systems with eight inputs (i.e. $X = [x, \dot{x}, y, \dot{y}, \theta_1, \dot{\theta}_1, \theta_2, \dot{\theta}_2]^T$) and one output. Each of these fuzzy systems approximates one of the control signals (15).

The fuzzy approximators are created using the approach introduced in [10].

First, N_i normal, complete, and consistent triangular membership functions $A_i^1, ..., A_i^{N_i}$ are created on the each of the inputs' domains $[\alpha_i, \beta_i]$:

$$\begin{aligned} &\mu_{A_i^1}(x_i) = \mu_{A_i^1}(x_i; e_i^1, e_i^1, e_i^2) \\ &\mu_{A_i^j}(x_i) = \mu_{A_i^j}(x_i; e_i^{j-1}, e_i^j, e_i^{j+1}),\ j \in \{2, ..., N_i - 1\} \\ &\mu_{A_i^{N_i}}(x_i) = \mu_{A_i^{N_i}}(x_i; e_i^{N_i-1}, e_i^{N_i}, e_i^{N_i}) \end{aligned} \quad (18)$$

where $\alpha_i = e_i^1 < e_i^2 < ... < e_i^{N_i} = \beta_i$ and e_i^j is the center of membership function A_i^j.

Next, $\prod_{i=1}^{8} N_i$ fuzzy IF-THEN rules are created in the following form:

$$Ru^{i_1...i_8} = IF\ x_1\ is\ A_1^{i_1}\ and\ ...and\ x_8\ is\ A_8^{i_8}, THEN\ y\ is\ B^{i_1...i_8} \quad (19)$$

where $i_j = 1, ..., N_j$ and the center of the fuzzy set $B^{i_1...i_8}$, denoted by $\bar{y}^{i_1...i_8}$, is chosen as:

$$\bar{y}^{i_1...i_8} = u_1(e_1^{i_1}, ..., e_8^{i_8}) \quad (20)$$

Note that in the above equation it was assumed that the approximator is desired to estimate the nonlinear control signal u_1.

Last, a fuzzy system is constructed from the $\prod_{i=1}^{8} N_i$ rules of (19) using product inference engine, singleton fuzzifier, and center average defuzzifier:

$$f(x) = \frac{\sum_{i_1=1}^{N_1} ... \sum_{i_8=1}^{N_8} \bar{y}^{i_1...i_8}(\mu_{A_1^{i_1}}(x_1)...\mu_{A_8^{i_8}}(x_8))}{\sum_{i_1=1}^{N_1} ... \sum_{i_8=1}^{N_8} (\mu_{A_1^{i_1}}(x_1)...\mu_{A_8^{i_8}}(x_8))} \quad (21)$$

The accuracy of this fuzzy system can be computed using Theorem 10.1. in [10]:

$$\| u - f \|_\infty \le \tfrac{1}{8}[\| \tfrac{\partial^2 u}{\partial x_1^2} \|_\infty h_1^2 + ... + \| \tfrac{\partial^2 u}{\partial x_8^2} \|_\infty h_8^2] \quad (22)$$

where $h_i = \max_{1 \le j \le N_i - 1} | e_i^{j+1} - e_i^j |$ for $i = 1, ..., 8$.

In this paper, h_i were chosen so that the fuzzy approximator was able to approximate the control signals with an accuracy of 0.01.

V. Experimental Results

Fig. 6 illustrates the way different parts of the ball and plate system are connected to each other. A PC was used to play the role of the controllers discussed in the last section. The inputs to the computer include the position of the ball (x, y) and the actuators angles (θ_1, θ_2). The former is extracted using image processing from the picture grabbed via a webcam and the latter is acquired from the encoders. Each encoder is mounted on a shaft which is connected to one of the stepper motors via a gearbox. The pulse generated by the encoders is read using ADVANTECH PCI-1753 data acquisition card to calculate the angles. The resulting control

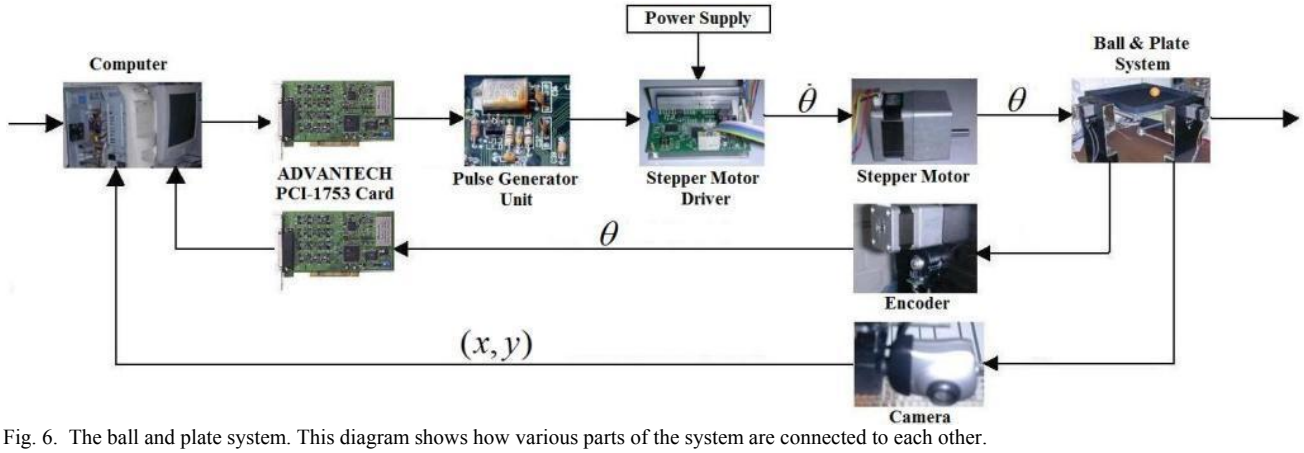

Fig. 6. The ball and plate system. This diagram shows how various parts of the system are connected to each other.

signals are set as the outputs of the data acquisition card.

The Pulse generator unit uses these outputs to create pulses with proper frequencies, which are sent to the drivers of the stepper motors.

Fig. 7 illustrates tracking a square of width 0.2 m, which is positioned symmetrically on the plate. The ball was initially located around the center of the plate. The results show that the PID controller equipped with supervisory fuzzy controller achieves a fast and monotonic response with respect to the PID controller with no supervisory control.

The result of position control using sliding control technique is shown in Fig. 8. The ball's initial location was (9,-5) cm. The controller was able to stabilize the ball on the center of the plate within a reasonable time and with great accuracy. The proposed sliding controller promises excellent performance in tracking control, which is the subject of future work.

VI. Conclusion and Future Works

In this paper the mechatronic design and control of a ball and plate system was discussed. Two controller schemes were proposed. The first one was based on a supervisory fuzzy system and PID controllers. The second one was based on sliding control with a fuzzy approximator. Experimental results corroborate the validity of these control strategies.

Implementing other control techniques, such as adaptive control and neural networks, to this ball and plate system and tracking more complex paths are the subjects of future works.

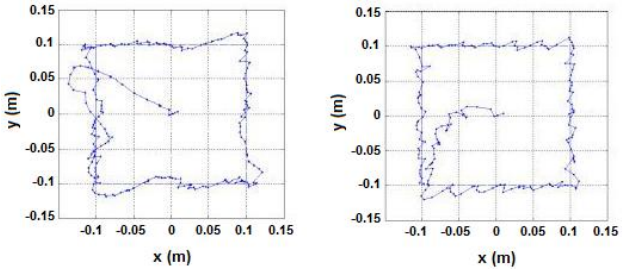

Fig. 7. Tracking a square of width 0.2 m: (a) without supervisory control and (b) with supervisory control. Each solid dot represents a data grabbed by the camera.

References

[1] O. Mohareri, and M. Saadat, "A new approach in designing ball and plate system, a mechatronic benchmark," In *Proc. 4th International Symposium on Mechatronics and its Applications*, Sharjah, UAE, 2007.

[2] S. Awtar, K. Craig, "Mechatronic design of a ball on plate balancing system," *Mechatronics*, 2002, vol. 12, no. 2, pp. 217-228.

[3] http://www.eissq.com/BallandPlate/index.html

[4] J. Park, Y. Lee, "Robust visual servoing for motion control of the ball on a plate," *Mechatronics*, 2003, vol. 13, no. 7, pp. 723-738.

[5] HUMUSOFT CE151 ball and plate apparatus users manual.

[6] H. Wang, Y. Tian, Z. Sui, X. Zhang, and C. Ding, "Tracking control of ball and plate system with a double feedback loop structure," In *Proc. 2007 IEEE International Conference on Modeling and Automation*, Harbin, China , 2007.

[7] M. Bai, H. Lu, J. Su, and Y. Tian, "Motion control of ball and plate system using supervisory fuzzy controller," In *Proc. 6th World Congree on Intelligent Control and Automation*, Daliian, China, 2006.

[8] E. Samson, D. Laurendeau, M. Parizeau, S. Comtois, J. Allan, and C. Gosselin, "The agile stereo pair for active vision," *Machine Vision and Applications Journal*, 2006, vol. 17, no. 1, pp. 32-50.

[9] J. Craig, *Introduction to Robotic: Mechanics and control*. Pearson Education, 2005, ch. 3.

[10] L. Wang, *A Course in Fuzzy Systems and Control*. Prentice-Hall PTR, 1997, ch. 20.

[11] J. Slotine and W. Li, *Applied Nonlinear Control*. Prentice-Hall, 1991, ch. 7.

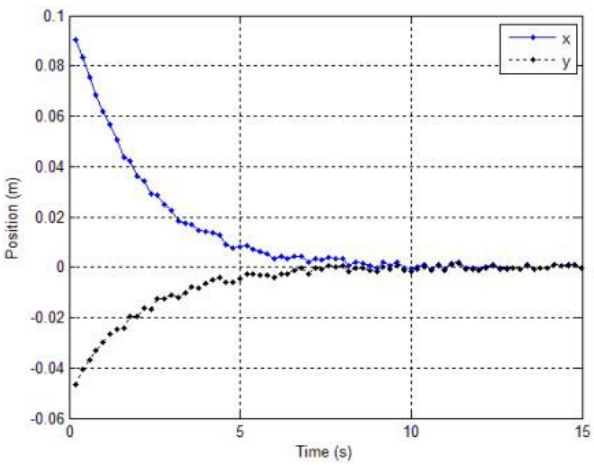

Fig. 8. Position control using sliding control technique. Each solid dot represents a data grabbed by the camera.